TASC

Theory and application of the Track Age Spectra Calculation

David X. Belton
The University of Melbourne, 2005

Contents

Track Age Spectra Calculator: using a length-calibrated age equation to build time lines into fission track length distributions

Summary

TASC is a method for gaining additional information from the raw track length and apparent age data routinely collected for fission track samples. The observed track lengths are de-biased using established methods and provide the input to calculate a "true" track density from the observed density. Length-dependent observation probabilites are incorporated into the fission track age equation thus providing the absolute age of the oldest measured or retained track – the "cooling onset" age. Since, to a first approximation, short tracks are older than long tracks, each track length can be allocated an equivalent age, thus allowing the traditional track length histogram to be recast as a "track age spectrum" in which each bin represents a finite span of real time. As well as extracting a "cooling onset age" the spectrum provides an age-length correlation for the full track length distribution; so that it adds an all-important time line to the traditional interpretation of track length histograms. The time information is quantitative - with an indication of age uncertainties - and the calculation is independent of chemistry and mineralogy, though subject to anisotropy. The temperature information is largely qualitative. Contemporary inverse modelling techniques test many thousands of plausible and implausible solutions and can include additional independent constraints to improve the fit between the mathematically acceptable solution and the geologically realistic history. The track age spectrum can therefore provide a very useful guide to the complex thermal histories before inverse modelling is attempted thus improving the convergence of modelling and minimising the number of non-unique solutions. Robust thermal histories can be rapidly developed, particularly in shield areas where stratigraphic control may be absent. Although primarily considered for apatite, the method may also prove of significant value in the study of other minerals such as zircon or sphene, where fission track annealing models are still evolving. This work describes the theoretical and practical foundations of a concept first presented at the International Conference on Thermochronology in Amsterdam (Belton et al., 2004).

1.1 Introduction

It has long been accepted practice in the fission track community to interpret apparent fission track ages as mixed or thermally-modified ages. With few exceptions, the ages do not identify geologically significant events. Furthermore, thermochronologists have recognised that the application of such age data to geological problems can only be undertaken in association with a confined track length distribution from the same sample which reflects the style of thermal variations to which the sample has been subjected (Gleadow et al., 1986). Over the last decade, this has typically involved various approaches utilising thermal history modelling.

However, early fission track researchers tended to adhere to the "closure temperature" concept widely applied to high temperature thermochronology (Naeser and Faul, 1969; Dodson, 1973; Haack, 1972; James and Durrani, 1986). This view was gradually modified by recognition of the effect that track fading has on the measured age (eg. Wagner and Reimer 1972). Prior to the advent of powerful inverse modelling methods (eg. Corrigan, 1991; Lutz and Omar, 1991) and predating the development of the early forward models, attempts were made to "correct" for track fading. For some time, researchers had been aware of the extreme sensitivity of tracks in apatite to temperature that implied continued annealing even at temperatures below 50ºC (Green, 1980). More importantly, they were beginning to understand the impact this observation had on fission track ages (Storzer and Wagner, 1969).

To address this problem a number of solutions were proposed, including the glass-plateau method (Carpena et al., 1980; Chaillou and Chambaudet, 1981) and the track length correction (Storzer and Wagner, 1969; Wagner and Storzer, 1972; Nagpaul, 1974). Fleischer et al. (1975) present a summary of the principles of several "correction" methods. With some notable exceptions, corrected ages rarely yielded geologically meaningful results and as a result not all researchers agreed with these methods (Boellstroff, 1981). Often it was unclear precisely what was being corrected (Gleadow et al., 1986) and by the mid-90's the correction procedure had all but disappeared from published fission track research (cf. Burtner et al., 1994). The advent of sophisticated inverse modelling techniques (eg. Gallagher, 1995) and readily available software for implementing them (eg. Crowley, 1993; Issler, 1996; Ketcham et al., 2000) made the age "correction" concept essentially redundant.

One of the problems with the application of the track length "correction" in the past may have been the use of *mean* track length of natural samples with complex thermal histories. While both the mean and standard deviation are established parameters for

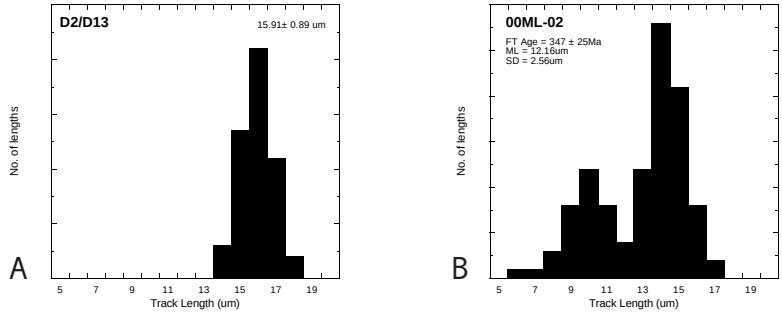

Figure 1 Examples of the variation in fission track length distributions both described in terms of their mean value and standard deviation. A) Synthetic sample an induced sample (mean length = 15.91µm, std. deviation = 0.89µm) used by Green in his mixing experiment (Galbraith et al., 1990). B) Natural sample (mean length = 12.16µm, std. deviation = 2.56µm) with a complex thermal history from Lorencak et al. (2004).

describing populations of track length measurements, it is clear that the mean value becomes increasingly imprecise as the measurements moves further away from the Gaussian distribution represented by an induced track length distribution (Fig. 1A) that a given example might lie. As a result, the mean track length (and the standard deviation) in a bimodal distribution, for example, (Fig. 1B) are both statistically imprecise and geologically vague in their representation of the complex underlying thermal history.

For this reason, it is proposed here that a more accurate representation of the age of the oldest track (ie. the time of earliest track retention) in a sample might best be determined by including in the standard age equation (Hurford, 1990) an integrated value that takes account of the individual peculiarities of any given track length distribution. This is not a retrograde step back to age "correction" as it might at first appear. Rather, as is demonstrated below, there is more information to be derived from a fission track age and its track length distribution, than is presently available.

1.2 Review of the age equation

Apatite fission track ages are calculated using an equation not dissimilar to that routinely used in isotopic dating techniques, namely:

$$t_{apparent} = {}^{1}\!/_{\lambda_D} \ln\left[1 + \zeta\lambda_D\left(\frac{\rho_s}{\rho_i}\right)\rho_d\right] \qquad (1.1)$$

Within this equation, (λ_D) = the total decay constant, (ρ_s) = the number of spontaneous tracks in the sample, (ρ_i) = the number of induced tracks in an external detector, while the parameter zeta (ζ) is an empirical calibration factor (Hurford & Green, 1983):

$$\zeta = \frac{\phi \sigma I_r}{\lambda_F \rho_d}. \qquad (1.2)$$

Here, (ϕ) is the neutron fluence, (σ) is the thermal neutron cross-section for ^{235}U, (I_r) is the isotopic ratio ^{235}U/^{238}U, (λ_F) is the spontaneous fission decay constant and (ρ_d) is the number of tracks induced by a dosimeter glass. Previously, the length (or range) ratio (L_s/L_i) and the registration efficiency ratio (η_s/η_i) were explicitly included in the age equation quoted by Fleischer et al. (1975),

$$t_{apparent} = {}^{1}\!\!\diagup\!\!_{\lambda_D} \ln\left[1 + \left(g \frac{\sigma B I}{\lambda_F} \frac{L_s}{L_i} \frac{\eta_s}{\eta_i}\right) \lambda_D \left(\frac{\rho_s}{\rho_i}\right) \rho_d\right]. \qquad (1.3)$$

However, as Green (1985) noted, these ratios are traditionally considered to be unity, implying that the probability of measuring spontaneous lengths is equal to the probability for the induced tracks, and that they have equal registration efficiency. The issue of registration efficiency will not be pursued further here, but Green (1989) argued persuasively that the track length simplification could legitimately be applied to typical zeta standard samples (eg. Durango, Fish Canyon) and equally as well to other "undisturbed" volcanic samples of unknown age. The matter of annealed samples with shorter lengths was largely dismissed with the acceptance that the "fission track age will be correspondingly reduced" (Green 1989, p349).

The aim of this work is to demonstrate that the importance placed by Fleischer and his colleagues (1975) on the length ratio was valid. By including an adaptation of the length ratio (L_s/L_i) in the traditional age equation, we produce a "length-calibrated age" that can be interpreted as the age of the oldest retained fission track. Since in real samples the spontaneous lengths (L_s) are neither a single value nor, with few exceptions, are they equal to the induced length (L_i), ages calculated using the assumption of (L_s/L_i) =1 in Eq. 1.1 (and Eq. 1.3), will be an underestimate of the ratio. In order to recalibrate the "age" to reflect the true population of tracks, the length ratio needs to be scaled by a factor which reflects the difference between

$$\frac{L_s}{L_i} \quad \text{and} \quad \frac{\int f(L_s) dL_s}{L_i}, \qquad (1.4)$$

where $\int f(L_s) dL_s$ is the integration of lengths in the true track length distribution. Using this approach, valuable insights can be gainedfrom the combination of both the age information and the track length data. Thus the way fission track age data and the information available are treated can be reassessed.

1.3 Assumptions in the length-calibrated age

Calculation of a length-calibrated age presupposes two important conditions: 1) that the true length distribution of tracks within the solid is known; and 2) that there is a characteristic (in this case linear) relationship between the track length and the density of tracks intersecting the surface upon which the age determination is based.

1.3.1 On the true length distribution of tracks in the solid

In addressing this first condition, the work of Laslett et al. (1982) provides guidance. In this work it is argued that horizontally confined tracks, combining both TINTS and TINCLES (Lal et al., 1969), provide the closest representation of the *true* track length distribution. While they noted that all raw observations are inherently biased, the analysis by Laslett and co-workers (1982) demonstrated that in the case of horizontally confined tracks, it is easy to apply a correction. However, the strong anisotropy of apatite also influences the observed track length, with the result that tracks near to parallel with the c-axis are invariably longer than those approaching the orthogonal (Green et al., 1986). More significantly, this anisotropy increases in tandem with increased annealing (Donelick et al., 1999). For this reason the comment in the summary above that "short tracks are older than young tracks" is very clearly "a first approximation". However, Donelick et al. (1999) demonstrated how a population of tracks can be projected onto the c-axis as a means of normalising the lengths. In the absence of such a correction, anisotropy is the main contributor to the increasing standard deviation observed in laboratory experiments (Fig. 2). The calculations described below do not explicitly correct for anisotropy, instead, the standard deviation is incorporated as a means of quantifying age uncertainty due to anisotropy on the spectrum results. If an oriented and corrected data set are used in the calculation, the raw histogram binning will vary but the ages remain unchanged and the errors assigned become overly conservative.

1.3.2 On the relationship between track length and density

The interplay between fission track length and the density of etch pits representing track intersections with a polished surface has had considerable attention from researchers (Wagner and Storzer, 1972; Nagpaul et al. 1974; Green 1980, 1988) and as pointed out by Laslett et al. (1984), the early efforts produced conflicting results. One of the key conclusions of Green (1988) was that the influences of sample bias and annealing anisotropy played a key role in disguising the true relationship. The experimental work by Green (1988) confirmed the linear relationship was unhindered by these influences for $l/l_o > 0.6$. In their study Laslett et al. (1984, p29) noted that the fission track equations "imply that the mean length of fission tracks should be proportional to their density". They went on to

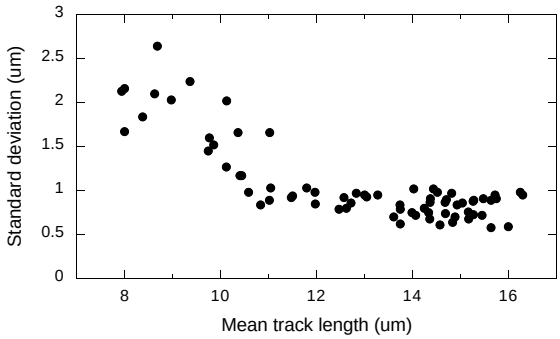

Figure 2 Standard deviation versus mean length in annealed Durango samples. (after Green et al., 1986).

show that in order to achieve a best fit, it was necessary to correct for both anisotropy due to crystallographic orientation and observational biases. This they did using a *length factor (L^*)* which accounts for the track angle with the c-axis. Their results using L^* support a linear relationship between length and density. Using a different approach to dealing with essentially the same problem, Donelick and his co-workers (1991, 1999) presented their elliptical model which fits a population of orientated, confined tracks to a ellipse that describes the natural variation in both thermal annealing and etching characteristics in a grain. Significantly, the approach of Donelick et al. (1999) also resulted in a nearly flat trend in the standard deviation of the lengths with a value of ~0.5µm, in contrast to that shown in Fig. 2. In the work reported on here, length bias was accommodated and an allowance made for the effects of anisotropy, enabling the linear relationship between track length and track density (and its age implications) to be usefully exploited.

1.4 A framework for the track age spectra calculation (TASC)

Bearing in mind the caveat on anisotropy, we return to the *approximation* that short tracks are older than long tracks. In a natural sample, the most recent tracks, with the least exposure to the variables of time and more importantly temperature, are at their longest (ie. approximately *initial* - l_o) length. In contrast, the shortest track results from integration of the time since its formation and the temperatures the rock has seen over that span of time. For a young, long and an old, short track in the same crystal, this model would forbid the longer track ever annealing to the point where it is shorter than the old track. Though in practice a level of uncertainty is allocated to the individual lengths/bins that permits this condition to be broken - ie. annealing anisotropy. The model does however, hold for samples in which the tracks have been adjusted for orientation and anisotropy using the approach of Donelick et al. (1999). If the ^{238}U fission events that produced the tracks are assumed to occur continuously and at nominally equal intervals in time, then each retained track length can be allocated an equivalent age ranging from the present

(~0Ma) for the longest track to a maximum representing the age of formation of the shortest (oldest) retained track. As a consequence, each bin of the traditional track length histogram can be allocated to a specific time interval, hence recasting the histogram in the form of a "track age spectra".

1.4.1 Defining the initial track length (l_o)

In each of a series of detailed annealing studies using induced ^{235}U tracks, the initial length (l_o) was determined as the mean of the induced tracks (Green et al., 1986; Crowley et al., 1991; Carlson et al., 1999, Barbarand et al., 2003). All subsequent annealed lengths (l) were compared against this mean value to calculate the reduced length (l/l_o). This is clearly a valid procedure since all the tracks were formed at approximately the same instant in the nuclear reactor, have suffered minimal annealing (cf. Donelick et al, 1990) and their nominally Gaussian distribution is a function of the mass/energy variation in fission products (Crowley, 1985) and some minor observational bias, anisotropy, and measurement error (Green, 1988). Effectively, the central value or mean length is the most representative value of the inital length. In the case of Durango apatite, the initial length could be accepted as ~16.3µm (Gleadow et al., 1986).

In contrast, spontaneous ^{238}U track length distributions in natural samples - even "undisturbed" volcanics (Gleadow et al., 1986) (ie. never reheated) - are very different. They may have what appears to be a nominally Gaussian distribution but these tracks have been formed at approximately even intervals (perhaps 10^5, 10^6 or more years apart) and have each been subject to annealing (at ~25ºC in undisturbed volcanics) for progressively longer periods of time. As a result, the track most likely to approximate the initial length is the youngest, most recently formed track. The longest, single track in the observed distribution for natural spontaneous tracks has the highest probability of being the youngest. In effect, as each track is formed, it samples the distribution described above for induced tracks, once only, and then begins the slow process of annealing. So while the mean length for spontaneous tracks in Durango, might be measured at 14.24µm (Green, 1988), the maximum track length in the distribution is the value most likely to approximate the actual initial length (l_o) - in this case ~16.3µm. Thus for the purposes of the track age spectra calculation (TASC), the maximum measured length in raw length data (assuming a statistically reasonable number of tracks - eg. 100) is considerd to be the initial length (l_o) of all the tracks. For binned data, a default value of 16.3µm may therefore be used.

1.4.2 Length distribution and observational probability

If the linear relationship between track length and track density in a polished surface discussed above is accepted, then it is instructive to following the logic of Laslett et al.

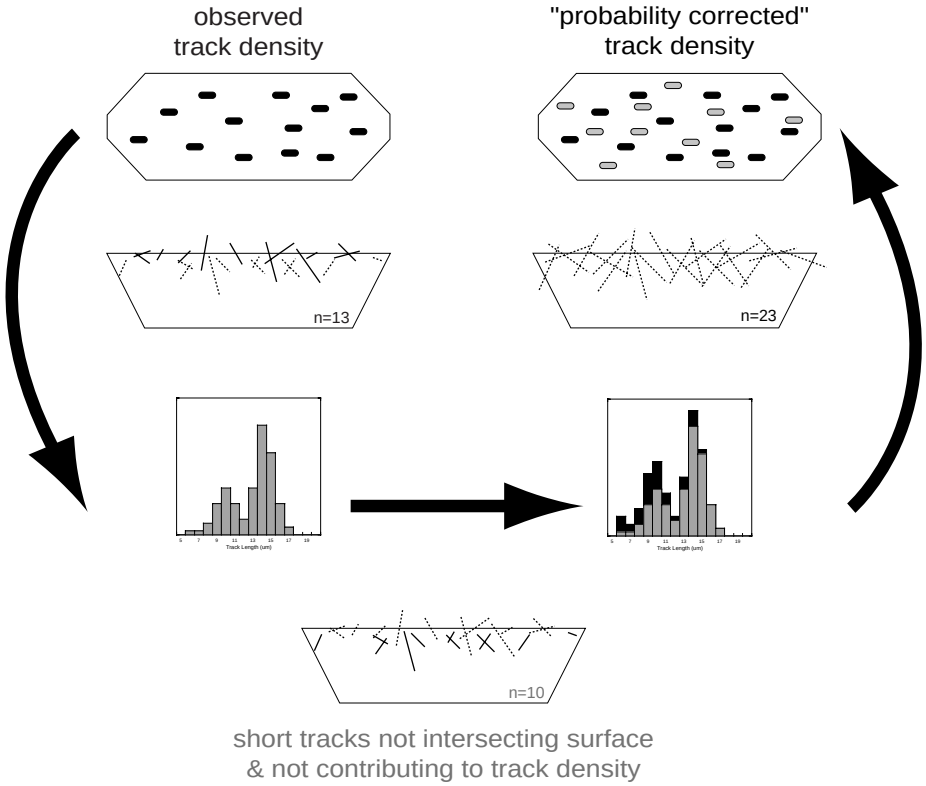

Figure 3 General concept of the length-calibrated age calculation. By utilising all the information available to us in the measured length histogram, the traditional apparent age can be recast in a form that has a specific geologic meaning ie. the age of the oldest retained track which, in basement samples, is equivalent to the time of entry into the base of the partial annealing zone (PAZ).

(1982) who estimated the probability of a track intersecting an arbitrary surface through a grain. They concluded that the sampling or intersection probability is directly proportional to the track length (ie. the linear length-density relationship). Their argument was, in essence, that a 16µm track is twice as likely to be sampled (or intersect the surface) as an 8µm track and 4 times as likely to be sampled as a 4µm track. Laslett et al. (1982) also provided a mathematically rigourous assessment of the spherical case, amongst others, applied to TINTS and TINCLES (Lal et al., 1969).

The inverse of the Laslett et al. (1982) argument is: that for a given "true" or debiased track-length distribution, the "true" number of 8µm tracks that would have intersected the surface at formation length (l_o in this case ~16µm), will be the observed amount multiplied by 2, since because of the processes of annealing, there is only a 50% probability of measuring the shortened track. Similarly, the "true" number of 4µm tracks will be the observed amount multiplied by 4 to adjust for the observation probability of only 25%. This correction is equivalent to extending all tracks in a variable length distribution back to their initial formation length (l_o). Once the true probability is determined for each

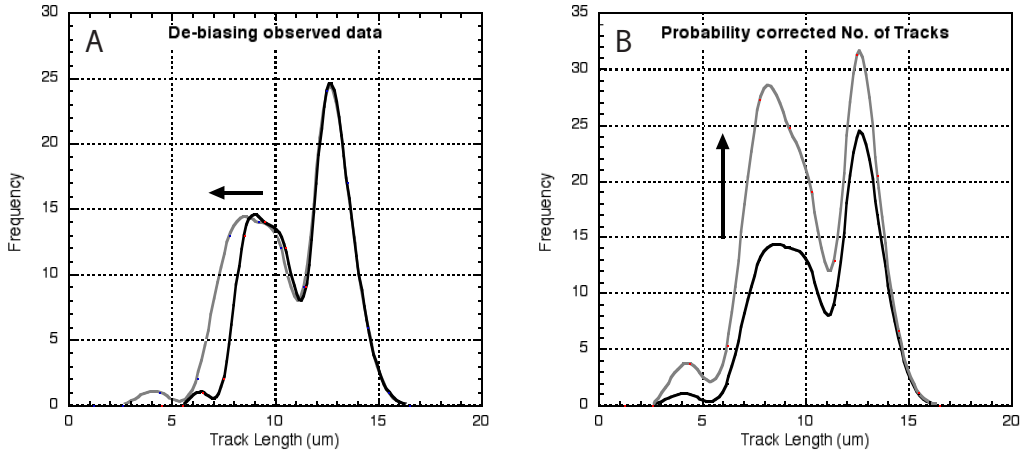

Figure 4 A) The measured track lengths are first de-biased to account for the fact that short tracks are less likely to intersect cracks or other tracks and thus be exposed to the etchant (after Laslett et al. 1982). This adjustment primarily effects the shorter tracks and in practice the variation for many younger samples is minimal. B) The de-biased lengths are then resampled using Eq. 2.7. As with the de-biasing function upon which it is based, re-sampling mainly affects shorter lengths. With the increase in length dispersion, re-sampling lengths below 5µm can generate very large errors. For this reason, 5µm was determined as a cut-off for input bin data.

individual observed length in the distribution (or each bin if only binned data are available) is determined, the total number of additional tracks that would be expected to intersect the surface are used to modify the L_s/L_i ratio from Eq. 1.3. A summary of the process is given in Fig. 3. This method ensures that the recalculated density of spontaneous tracks (ρ_s) in the polished surface reflects that observed distribution of tracks within the solid.

1.5 Calculating the "length calibrated age"

The first step is to debias the raw horizontal track length data using the approach of Laslett et al. (1982). Fig. 4 illustrates a typical example of the effect of this procedure. This is preferably undertaken with the individual length data, however binned data can be used - though with some loss of precision. Once de-biased, an estimate of the overall true intersection probability based on individual tracks can be made using l_o as the reference length:

$$N = \sum \frac{l_o}{l_m} \qquad (1.5)$$

Where N is the resampled value of full-length tracks, l_o is the initial track length and l_m is the measured length of each observed track. In practice, it is reasonably efficient to deal with the binned data data routinely collected and/or published for horizontal confined lengths. In this case, Eq. 1.5 can be recast as:

$$N_j(r_j) = n_j(r_j)\frac{l_{\max}}{l_j(r_j)} \qquad \text{and} \qquad N = \sum n_j(r_j)\frac{l_{\max}}{l_j(r_j)} \qquad (1.6, 1.7)$$

where N_j is the corrected count in the *jth* interval (bin) centred at r_j using the initial track length (l_o) and $l_j(r_j)$, the observed track length at r_j, to adjust the observed bin counts $n_j(r_j)$. The re-sampled total value of tracks N is now given by the summing each of the bins.

The length-calibrated age equation:

$$t^*_{cool-onset} = {}^{1}\!/_{\lambda_D} \ln\left[1 + \varsigma\lambda_D\left(\frac{\int f(L_s)dL_s}{L_i}\frac{\rho_s}{\rho_i}\right)\rho_d\right] \qquad (1.8)$$

is simplified to

$$t^*_{cool-onset} = {}^{1}\!/_{\lambda_D} \ln\left[1 + \varsigma\lambda_D\left(\frac{N}{n}\frac{\rho_s}{\rho_i}\right)\rho_d\right] \qquad (1.9)$$

since the term N/n is applied to correct for the difference between the observed track density (ρ_s) routinely calculated assuming (L_s/L_i) =1 and the adjusted fission track density calculated using Eq. 1.5-1.7. Thus the term N/n becomes a density (ρ_s) multiplier and may be used as a scale factor to directly modify the traditional age equation, Eq. 1.1. The resulting "length-calibrated" age will then reflect the "true" density of tracks (irrespective of track length reduction) retained since the sample entered the partial annealing zone.

Traditional fission track analysis using the external detector method involves approximately 20 grain ages being calculated separately prior to the application of statistics of central tendency (Galbraith, 1984). However, it is unlikely that a full track length distribution will be available for each individual grain, so under these circumstances, it may be appropriate to use a close approximation of the full age equation. This can be obtained by simply using the density multiplier (N/n) to adjust the apparent fission track age directly in the following manner:

$$t^*_{cool-onset} = t_{apparent}\left[\frac{N}{n}\right] \qquad (1.10)$$

This form is applied to the central age of the sample and ignores the exponential nature of the decay constant. Nevertheless, up to fission track ages of ~400Ma, the error on this approach is unlikely to exceed ~1% of the "length calibrated age", and is useful in rapidly determining the age intervals for each of the binned track counts.

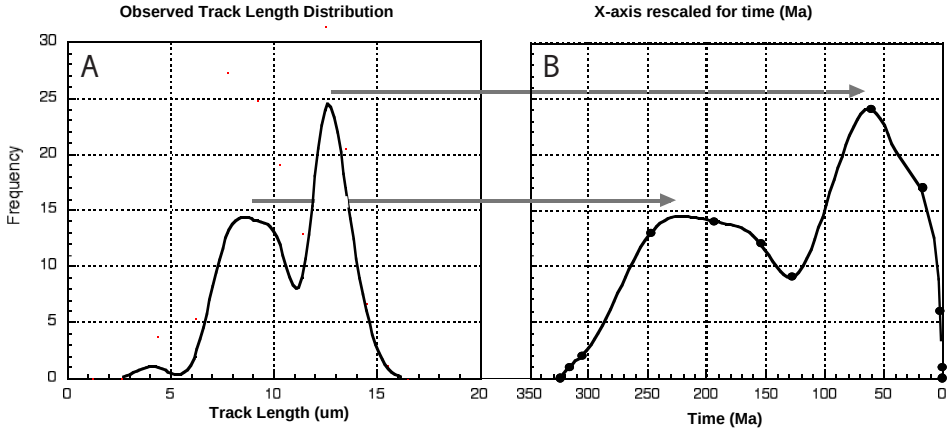

Figure 5 Once the "cooling onset" age has been calculated using Eq. 2.10, and the interval times determined for each length bin, the x-axis of the traditional histogram (A) can be recast onto a time-line as shown. This produces a track age spectrum (B) that retains all the thermal history information inherent in the original histogram but with the crucial addition of timing.

It should be re-emphasised at this point that the length-calibrated age is no longer an apparent age in the usual sense, it now represents the age of the oldest track remaining in the sample. The term "cooling onset" age will be used in the subsequent discussion to denote this calibrated age, recognising that while the nomenclature may be valid for samples that have been hotter than the partial annealing zone, it may occasionally be imprecise and potentially confusing in the case of sedimentary samples which may have had a protracted, near-isothermal history.

Once the "cooling onset age" has been determined, it is a simple matter to rescale the traditional length histogram with the relationship between the number of track lengths and the total number of "rescaled tracks" N (Fig. 5). Each bin is allocated its appropriate number of rescaled tracks (N_j) so that the boundary of each bin can be defined by a point in time. In order to allocate some measure of uncertainty (largely due to anisotropy) to the result, the entire procedure is carried out on the de-biased track lengths *minus* one standard deviation and again with the de-biased track lengths *plus* one standard deviation - based on the standard deviation observed in Durango by Green et al. (1986). This difference is combined (sum of squares) with the traditionally determined error on the apparent fission track age to give a plausible, though not necessarily statistically robust, estimate of the uncertainty of the bin ages. Where the track length data have been "corrected" for c-axis orientation (for example using the model of Donelick et al. (1999), then the errors attributed to each bin will be an over-estimate, since they are designed to accommodate the uncertainty in a data set that has not been adjusted for crystallographic anisotropy.

Recasting the traditional length histogram, using the age information derived above,

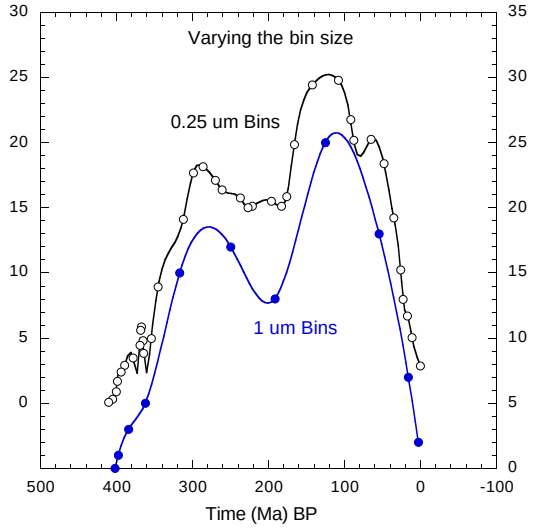

Figure 6 The track age spectra calculation described in the text has been undertaken using the routine 1µm bin data (lower curve-filled circles). If a smaller bin interval is selected, (eg. 0.25µm) as in the upper curve (open circles), a slightly more detailed plot results, however small variations in this curve may simply be attributable to the normal variations in track measurement and overinterpretation could result. At even smaller bin intervals the curve becomes too noisey to be useful. This suggests that a 1µm bin interval is probably optimal.

produces a plot that will subsequently be referred to as a "track age spectrum". The primary strength of this spectrum is that it retains all the original thermal history information from the length histogram - such as the skewed distribution of an accelerated cooling or the bimodality of a reheating event - but now enables the timing of these events to be readily estimated (see Fig. 6 regarding the effects of altering bin size). In the next section, the practical utility of the track age spectrum calculation (TASC) will be demonstrated using a variety of synthetic and real data sets.

1.6 Testing the TASC routine

1.6.1 Spectrum examples from synthetic histories

In order to test the spectrum calculation on geologically realistic samples, a series of synthetic histories were generated using the inverse modelling software MonteTrax (Gallagher, 1995). A number of arbitrary, but geologically plausible thermal histories were entered in order to generate the synthetic length histogram with an apparent fission track age and also the nominal age of the oldest track developed by the model (Table 1). The synthetic histories included: 1) linear cooling from 120ºC at 120Ma; 2) a saw-tooth style history with alternating phases of protracted cooling and heating before final exhumation; 3) similar to history [2] but with a rapid reheat/cool phase; 4) prolonged slow cooling in the PAZ with more recent accelerated exhumation; 5) early rapid exhumation

		Synthetic Model Data				TASC Output	
Synthetic sample	Thermal history style	FT age (Ma)	Mean (μm)	Std. dev. (μm)	Oldest track (Ma)	Cool onset Age (Ma)	ρ_s multiplier
MTX-02	linear cool	46	13.53	1.99	57	55 ± 4	1.19
MTX-05	prolonged reheat	91	12.70	2.04	114	115 ± 12	1.27
MTX-08	sharp reheat	81	12.45	2.40	114	108 ± 5	1.33
MTX-11	slow cool, modest acceleration	139	12.58	2.32	210	184 ± 20	1.33
MTX-12	rapid cool, shallow residence	93	14.23	1.57	100	104 ± 10	1.12

Table1 Summary of synthetic thermal histories generated using MonteTrax (Gallagher, 1995), and the TASC results for each. See Fig. 7 to Fig. 11 for the individual detail.

followed by a protracted period at shallow crustal temperatures.

Bin values from the synthetic histogram and the apparent fission track age were provided as input for the spectrum calculation, and the default initial length was 16.3μm. In each case, the track density multiplier (*N/n*) and the "cooling onset" age were calculated, and the length histogram was rescaled against time. An additional curve indicating the actual age contribution of each bin (calculated for the midpoint of the bin), and the estimated uncertainty of the nominal bin age was included. The age contribution curve emphasises the particular significance of shorter track lengths as a contribution to the overall history and occasionally identifies otherwise subtle variations in the traditional length histogram.

Subsequently, the output spectra were inspected to determine: 1) if the cooling onset age approximated the "age of the oldest track" in the original model; 2) whether or not the cooling onset represented the approximate time at which the model sample entered the base of the partial annealing zone; and 3) if the timing of "thermal events" (eg. acceleration/deceleration of exhumation, reburial and/or rapid cooling etc.) were identified.

1.6.2 Interpretation of the synthetic results.

1) MTX-02: the linear cooling spectrum (Fig. 7) forms something of a "standard" for interpreting more complex spectra. With the exception of the "undisturbed volcanic" style of history (see MTX-12 below), the linear cooling is perhaps the simplest and for many geological samples, probably represents the style of cooling for significant periods of their history. The contribution of shorter tracks in the skewed length histogram in Fig. 7 translates to an age spectrum in which the increasing contribution of successively longer tracks forms a curve approximating the Chi distribution. This general shape can be seen in samples with more complex histories - appearing perhaps two or more times, punctuated

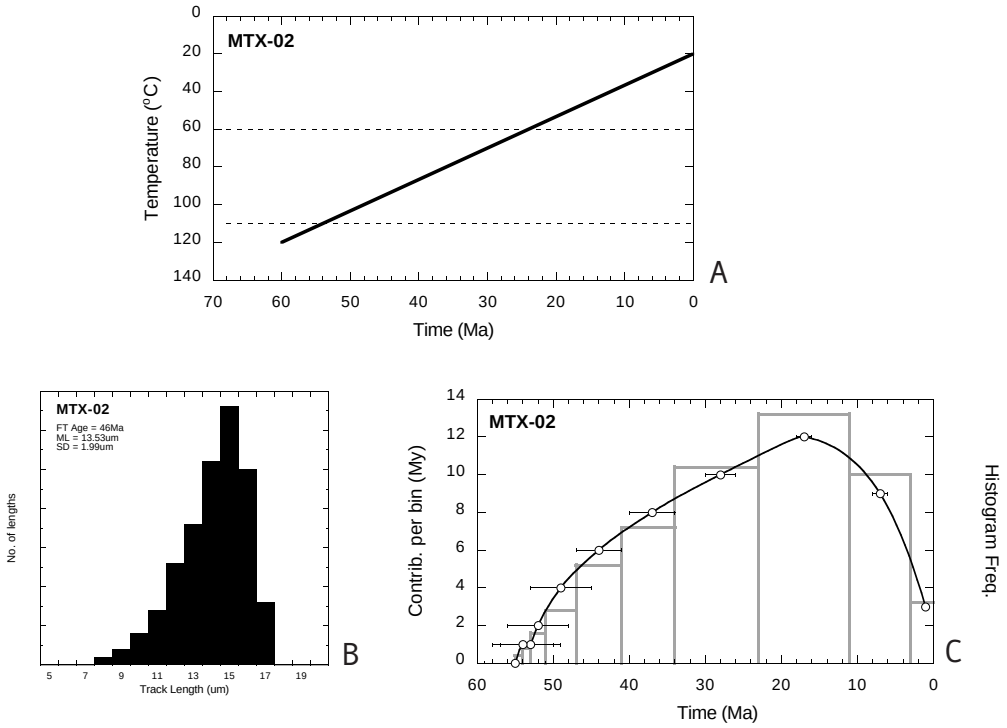

Figure 7 A) Synthetic thermal history for sample MTX-02 generated using MonteTrax (Gallagher, 1995). B) Traditional length histogram (mean length = 13.53µm, std. deviation = 1.99µm) for MTX-02. C) Track age spectrum for MTX-02 with age-mapped bins (grey) and the bin age-contribution curve shown with nominal uncertainties. Note that the two vertical axes are not at the same scale. See Table 1 for more details.

by a trough or saddle - the timing of which is coincident with changes in the thermal history.

2) MTX-05: This sample (Fig. 8) illustrates the combination of multiple "linear cooling" curves separated by a break associated with increased annealing due to reheating. It can be envisaged that this sample would have accumulated tracks in a manner very similar to MTX-02 above for its first 40My of linear cooling. Subsequent protracted heating acts to shorten the track length distribution en masse - effectively compressing the "linear style" curve to older end of the scale (ie. the left of the spectrum plot). During reheating, tracks continue to be accumulated but are rapidly annealed. Once the sample begins to cool again from 60 Ma, another "linear style" curve - consisting of longer tracks - is added to the distribution. In the case of a protracted reheat phase, the precise timing of maximum temperature is ambiguous, largely as a result of the continuous production of tracks acting to smooth out the transition between cooling phases.

3) MTX-08: Where a reheat phase is particularly rapid (in geological terms), the initial "linear cooling" component is pushed to the left of the plot (ie. shortened), but with

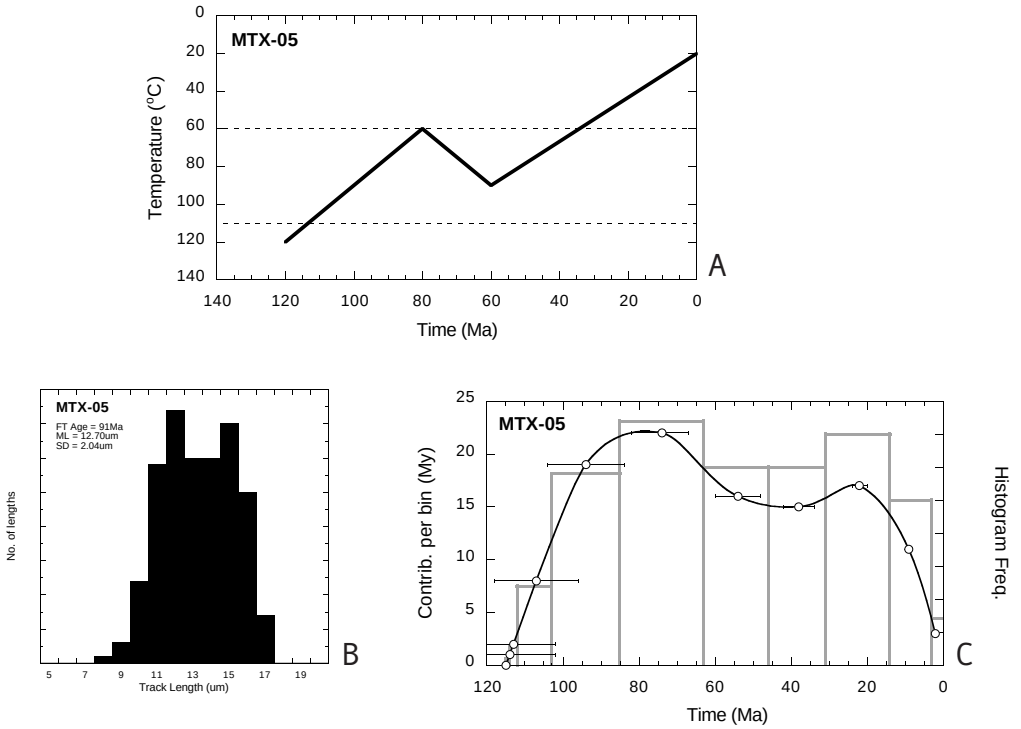

Figure 8 A) Synthetic thermal history for sample MTX-05 generated using MonteTrax (Gallagher, 1995). B) Traditional length histogram (mean length = 12.70µm, std. deviation = 2.04µm) for MTX-05. C) Track age spectrum for MTX-05 with age-mapped bins (grey) and the bin age-contribution curve shown with nominal uncertainties. Note that the protracted heating event acts to obscure the precise timing of maximum temperature. See Table 1 for more detail.

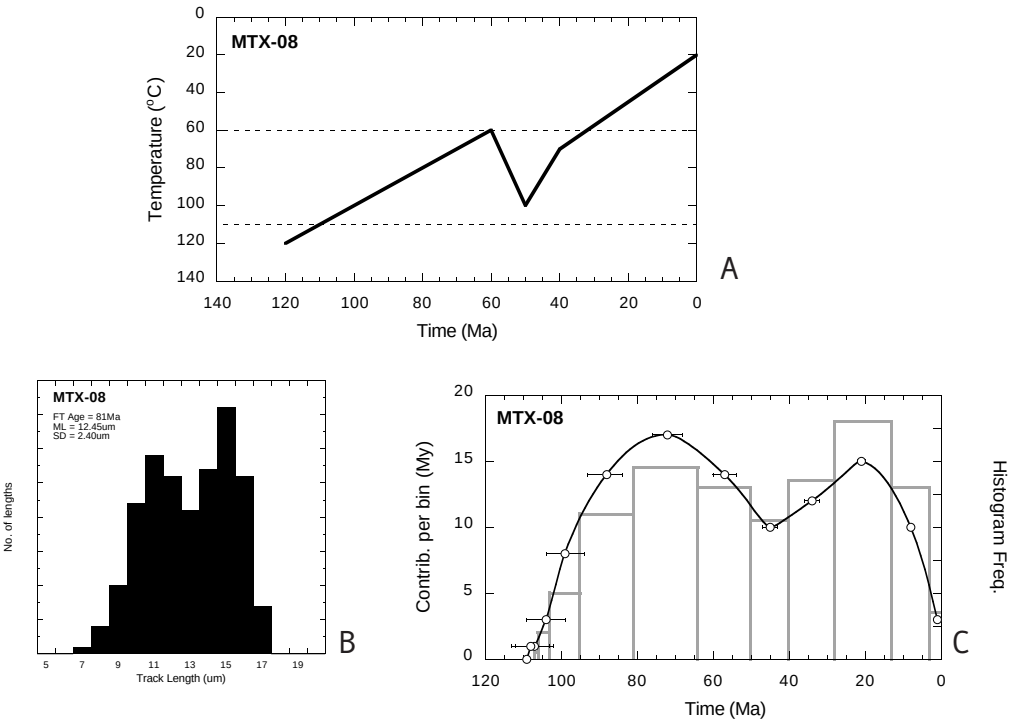

Figure 9 A) Synthetic thermal history for sample MTX-08 generated using MonteTrax (Gallagher, 1995). B) Traditional length histogram (mean length = 12.45µm, std. deviation = 2.40µm) for MTX-08. C) Track age spectrum for MTX-08 with age-mapped bins (grey) and the bin age-contribution curve shown with nominal uncertainties. Here, timing of the thermal perturbation is identified with reasonable precision. See Table 1 for more detail.

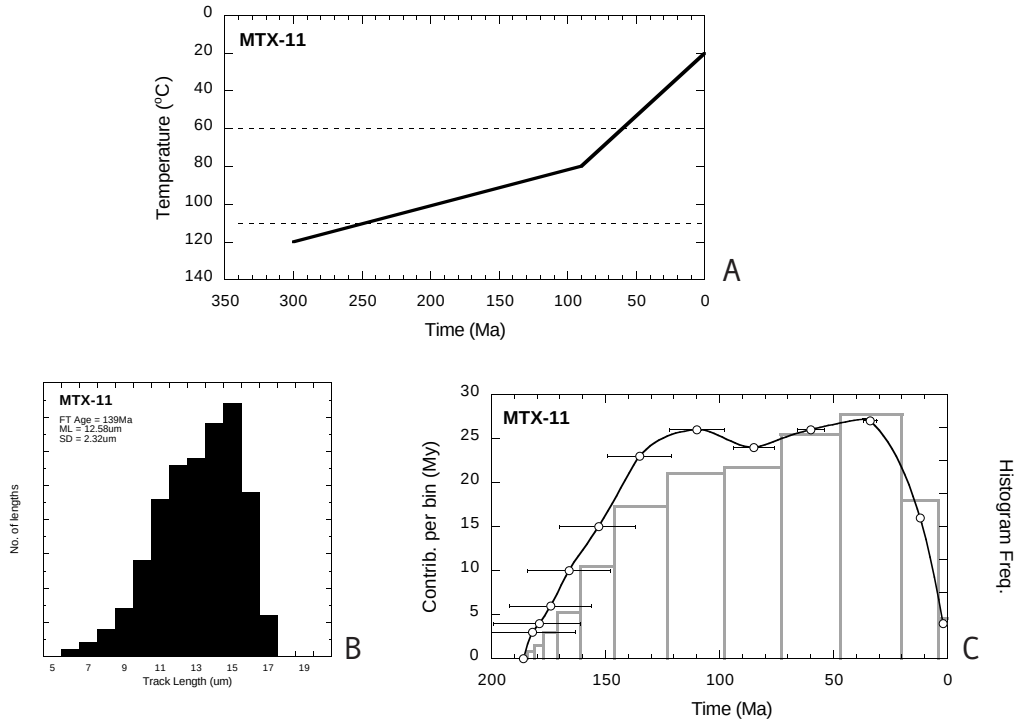

Figure 10 A) Synthetic thermal history for sample MTX-11 generated using MonteTrax (Gallagher, 1995). B) Traditional length histogram (mean length = 12.58µm, std. deviation = 2.32µm) for MTX-11. C) Track age spectrum for MTX-11 with age-mapped bins (grey) and the bin age-contribution curve shown with nominal uncertainties. Here, a relatively subtle change in the histogram is clearly visible in the age-contribution curve. See Table 1 for more detail.

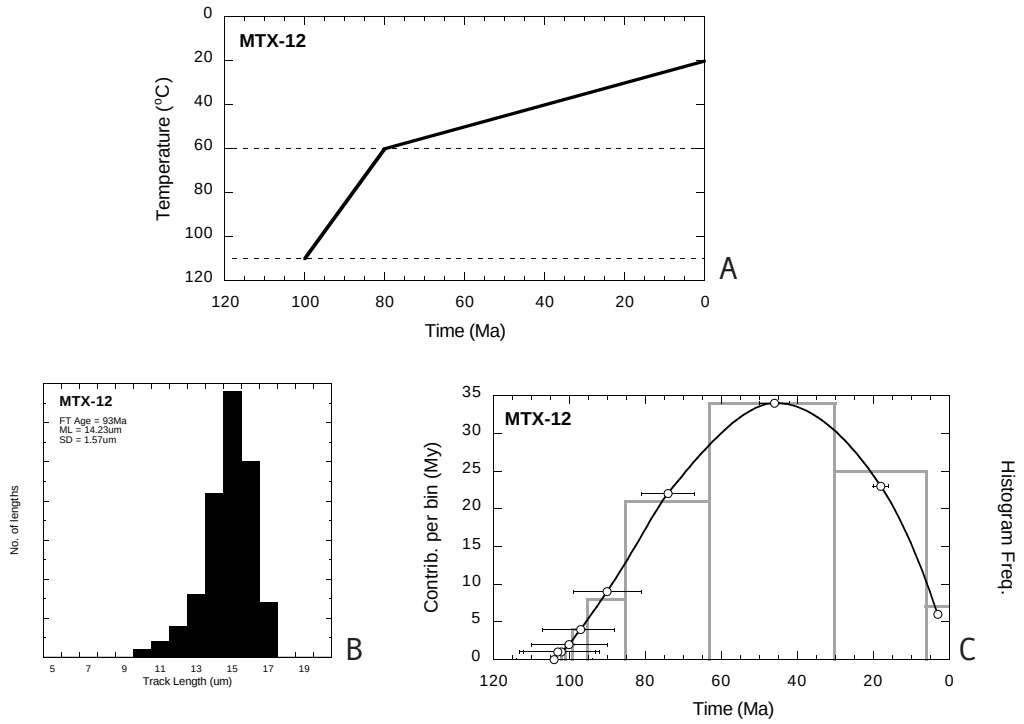

Figure 11 A) Synthetic thermal history for sample MTX-12 generated using MonteTrax (Gallagher, 1995). B) Traditional length histogram (mean length = 14.23µm, std. deviation = 1.57µm) for MTX-12. C) Track age spectrum for MTX-12. In this style of histogram, timing would appear to be marked by the large step between the 13mm and 14mm bins at ~85Ma. (see Fig. 2.10 for a natural example) See Table 1 for more detail.

a relatively brief duration of reheating, fewer tracks are produced during the period near the maximum reheat temperature (Fig. 9). Subsequent cooling re-establishes a new "linear cooling" component but with a much clearer transition. The timing of maximum temperature in this instance is more precisely defined than in the previous example.

4) MTX-11: As Gleadow et al. (1986) noted, truly bimodal distributions result under quite restricted thermal conditions. In contrast, phases of modest acceleration in cooling are rather more common. Expression of this phenomenon in a traditional length histogram is a skewed and broadened distribution (Fig. 10). However, the age spectrum in conjunction with the age contribution curve, provide a good indication of the timing of the change in cooling rate.

5) MTX-12: In the case of an "undisturbed volcanic" model, the traditional histogram has a clear unimodal distribution, characterised by long lengths and a narrow distribution (Fig. 11). Here, the age spectrum indicates the time of entry into the base of the PAZ (ie. the cooling onset age), but the timing of deceleration (at temperatures lower than the nominal PAZ) is not clear (timing in real samples generally seems to be less equivocal - see Fig. 8). Nevertheless, there is a clear distinction between this spectrum and that of a typical linear cooled sample (MTX-02 above) in that most of the age contribution in the volcanic model comes from only the longest lengths.

The value of the general approach described above, will become clear when used on real data from a variety of tectonic environments.

1.7 Field testing TASC

The spectrum calculations were also tested against real samples including several classic vertical profiles - the Mt Doorly profile in the Transantarctic Mountains (Gleadow and Fitzgerald, 1987), several Otway Basin wells (Gleadow et al., 1986b) and a zircon study from Crete (Brix et al., 2002). The first of these - the Mt Doorly Profile - illustrates the application of the track age spectra technique in elucidating a consistent timing of tectonic events from samples in the palaeo-PAZ as well as from below the "break in slope".

1.7.1 The Mount Doorly vertical profile (Gleadow and Fitzgerald, 1987)

A classic study from the Transantarctic Mountains by Gleadow and Fitzgerald (1987) provides an instructive example of the utility of the TASC approach (see results in Table 2). The Mt. Doorly profile consists of a sequence of basement apatites collected from a near-vertical section between 390m to 1200m. This profile formed the basis of an innovative interpretation of apatite cooling styles, in which the authors recognised the presence

Sample	Elevation (m)	FT Age (Ma)	Mean (μm)	Std. Dev. (μm)	Cool Onset Age (Ma)	ρ_s multiplier
R31735	1113	83 ± 7	13.21	1.81	102 ± 10	1.23
R31737	1041	64 ± 8	12.92	2.51	81 ± 13	1.40
R31739	856	50 ± 3	13.34	1.45	58 ± 8.7	1.16
R31741	671	49 ± 7	14.14	2.01	56 ± 8.2	1.15
R31743	485	47 ± 3	14.36	1.20	51 ± 3.3	1.09
R31744	393	48 ± 4	14.14	1.69	56 ± 4.6	1.16

Table 2 Summary of original fission track data from the Mt Doorly vertical profile in the Transantarctic Mountains (Gleadow and Fitzgerald, 1987), and the TASC results for each sample. See Fig. 12 to Fig. 14 for the individual detail.

of a “fossil” partial annealing zone. In the Mt Doorly example, this fossil PAZ had been rapidly exhumed, thus preserving the characteristic fission track age/elevation relationship frequently seen in borehole studies.

The track age spectra of samples from Mt Doorly offer some useful insigths into the tectonic history of this area. Samples that would have been resident in the crust at depths greater than the fossil PAZ appear below the “break in slope” in a traditional age elevation plot. The spectra for these samples (Fig. 12) consistently show some early track retention indicating a “cooling onset” age of ~55-50Ma. At about 40Ma, there is a dramatic increase in longer lengths resulting from an inferred rapid cooling event at that time. The distribution of this new track population tends towards an “undisturbed volcanic” shaped curve (discussed above) suggesting that the bulk of cooling/exhumation for the Mt. Doorly profile occurred at 40Ma and that the profile has been at or near the surface since that time.

The above interpretation is supported by the spectra from above the “break in slope” - ie. from samples within the fossil PAZ. These spectra show a progressive increase in both their apparent fission track age and the “cooling onset” age, consistent with a slow passage through the PAZ. Arguably, the increasing trend in “cooling onset” ages with elevation gives a better indication of the cooling rate than the “mixed” timing provided by traditional apparent age data, since the onset age marks the time at which the sample passed through a particular isotherm. More significantly, these spectra also retain critical timing information on the later rapid cooling step. Both samples above the “break in slope” have a marked trough in the age spectra at ~35-40Ma (Fig. 13), which coincides with the timing identified below the “break in slope”.

The nominal timing of such tectonic events as determined by the TASC approach (see all samples - Fig. 14) can be informatively summarised by means of an “event spectrum” (Fig. 15). This plot is analogous to the detrital zircon age-probability plots (Brandon,

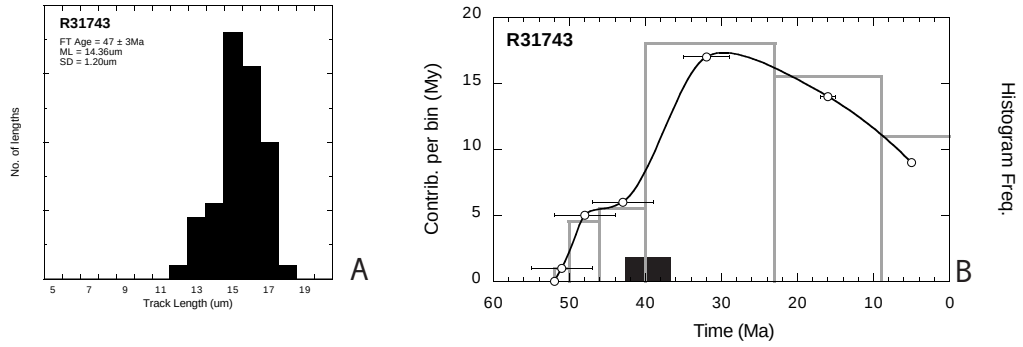

Figure 12 Mt Doorly profile, elevation - 485m, Sample - R31743 below the "break in slope". A) Traditional length histogram (mean length = 14.36µm, std. deviation = 1.20µm) C) Track age spectrum for R31737 shows a very clear thermal perturbation at ~ 40Ma denoted by the black zone. (Original FT data from Gleadow and Fitzgerald, 1987)

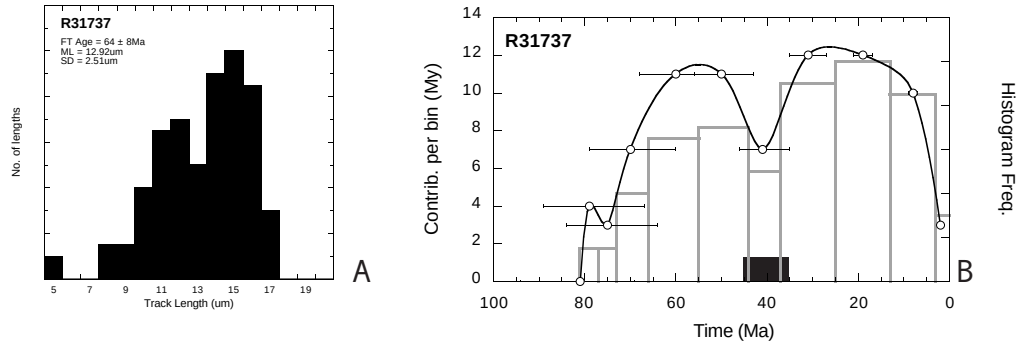

Figure 13 Mt Doorly profile, elevation - 1041m, Sample - R31737 above the "break in slope". A) Traditional length histogram (mean length = 12.92µm, std. deviation = 2.51µm) C) Track age spectrum for R31737 shows a very clear thermal perturbation at ~ 40Ma denoted by the black zone. (Original FT data from Gleadow and Fitzgerald, 1987)

Figure 14 (Overleaf) Mt Doorly profile, all samples elevation from 485m to 1119m. Track age spectra scaled to 120Ma for comparison. (Original FT data from Gleadow and Fitzgerald, 1987)

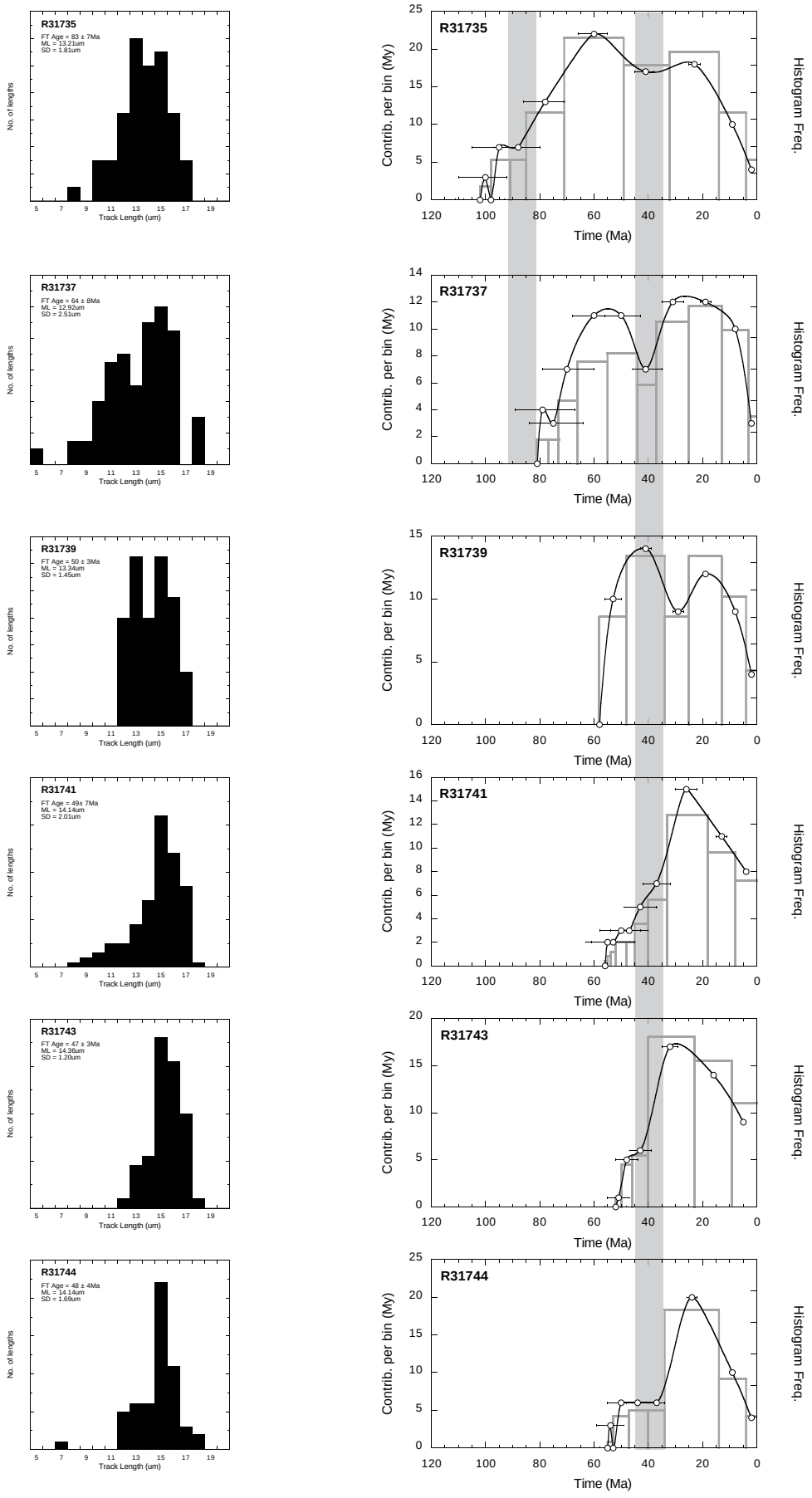
R31735
FT Age = 83 ± 7Ma
ML = 13.21um
SD = 1.81um
No. of lengths
Track Length (um)
R31735
Contrib. per bin (My)
Histogram Freq.
Time (Ma)
R31737
FT Age = 64 ± 8Ma
ML = 12.92um
SD = 2.51um
R31737
R31739
FT Age = 50 ± 3Ma
ML = 13.34um
SD = 1.45um
R31739
R31741
FT Age = 49± 7Ma
ML = 14.14um
SD = 2.01um
R31741
R31743
FT Age = 47 ± 3Ma
ML = 14.36um
SD = 1.20um
R31743
R31744
FT Age = 48 ± 4Ma
ML = 14.14um
SD = 1.69um
R31744

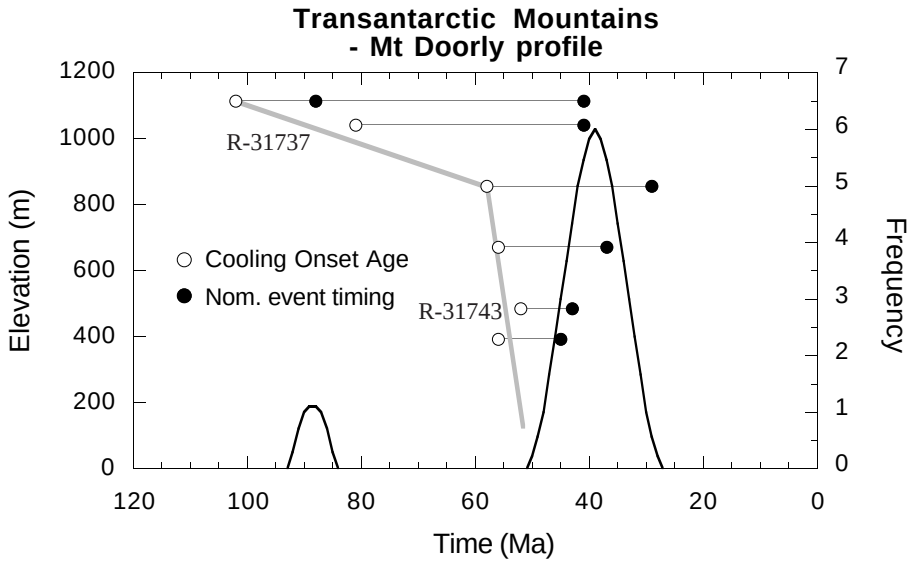

Figure 15 Event spectrum for Mt Doorly profile illustrating the significance of the "~40Ma" event in all the samples. Overlain on this is an age-elevation plot based on "cooling onset" ages - open circles, and nominal event timing in each sample - filled circles. The horizontal lines are intended to link onset and events for individual samples.

1996) seen in tectonic provenance studies. It is constructed by extracting the approximate timing of changes in cooling styles (as outlined in the synthetic model section) from the track age spectra. Since the timings are semiquantitative and generally imprecise, they are grouped to produce a nominal central value with some indication of dispersion. From this, a Gaussian curve is plotted using the calculated mean, the standard deviation, and the total number of samples from which the same timing has been observed provides the height of the curve. The intention of this plot is to indicate approximate time, with a crude determination of precision of this estimate and how widely this "event" might have been recorded in the sample set.

As a final point, it is worth noting that the uppermost sample in the Mt Doorly profile (R31735 at 1113m) records a step in the track retention at ~90Ma which is broadly coincident with the "cooling onset" age of the sample below (R31737 at 1041m).

1.7.2 The Otway Basin Wells (Gleadow et al. 1986b)

Largely because of its hydrocarbon potential, the Early Cretaceous Otway Basin of south eastern Australia has long been the focus of considerable research in thermochronology (Gleadow and Duddy, 1981; Gleadow et al., 1986b). The basin records the rifting and breakup of Australia's southern margin and is marked by the complex interplay of shear tectonics on graben and half-graben structures (Duddy, 2000). Its early rift-phase development is characterised by rapid deposition of terrigenous-fluviatile sediments and volcanogenic detritus covering the period 135-95Ma (Gleadow and Duddy, 1981) The samples

discussed here are from two important wells penetrating the Early Cretaceous sequences.

Table 3 summarises the results of TASC analysis on samples from Flaxmans-1 and the Port Campbell-4 wells in the Otway Basin. The first point to note is that all the samples from the Port Campbell-4 well and the upper two from Flaxmans-1 show a "cooling onset" age of around 113 ± 5Ma, which replicates the stratigraphic age of the Otway Group (Duddy, 2000). This unit is dominated by the Eumarella Formation, a volcaniclastic unit resulting from explosive (dacitic) volcanism over much of the Early Cretaceous. In this instance, the term "cooling onset" may be a little confusing though it nevertheless represents the point in time at which the sample began retaining tracks (ie. the time of eruption). From the apparent fission track ages and the track length data It is clear that time and temperature have acted to alter the form of the length distributions.

In the Port Campbell-4 well (Fig. 16), the least thermally effected sample (PC-1850m) retains what is essentially a modified volcanic signature. In contrast, PC-2411m has suffered considerably more annealing but has not been fully reset. The track age spectrum retains the same "cooling onset" age implying that no tracks have been completely annealed, but also records what appear to be two reheating events - one at ~100Ma, the later one at ~ 55Ma. The Cenomanian event is coincident with Duddy's (2000) inferred Mid-Cretaceous tectonism associated with opening of the Southern Ocean.

There is no evidence of this earlier event seen in the track age spectra of Flaxmans-1 (Fig. 17). Both wells, however, record the younger ~ Eocene? event which parallels the development of a basin-wide unconformity at about the time spreading in the Southern Ocean accelerated (Duddy, 2000). At depths below 2500m in Flaxmans-1 (temperatures

Sample	Depth (m)	FT Age (Ma)	Mean (µm)	Std. Dev. (µm)	Cool Onset Age (Ma)	ρ_s multiplier
Flaxmans-1						
87°C	2332	98	12.80	0.80	115 ± 11	1.17
89°C	2429	76	11.22	1.08	103 ± 7	1.35
92°C	2585	54	10.54	1.39	80 ± 8	1.48
108°C	3085	16	8.56	2.48	34 ± 13	2.75
Port Campbell-4						
73°C	1850	112	13.22	0.93	137 ± 13	1.22
87°C	2347	80	11.97	1.62	113 ± 12	1.41
89°C	2411	87	11.93	1.50	122 ± 14	1.41
93°C	2595	65	10.59	2.01	106 ± 18	1.88

Table 3 Summary of original fission track data from the Flaxmans-1 and Port Campbell-4 wells in the Otway Basin of south eastern Australia (Gleadow et al., 1986b), and the TASC results for each sample. The Otway Group ranges from ~135-95Ma within which the largely volcanoclastic Eumarella Formation has an outcrop age of 120Ma (Gleadow & Duddy, 1981). See Fig. 16 to Fig. 18.

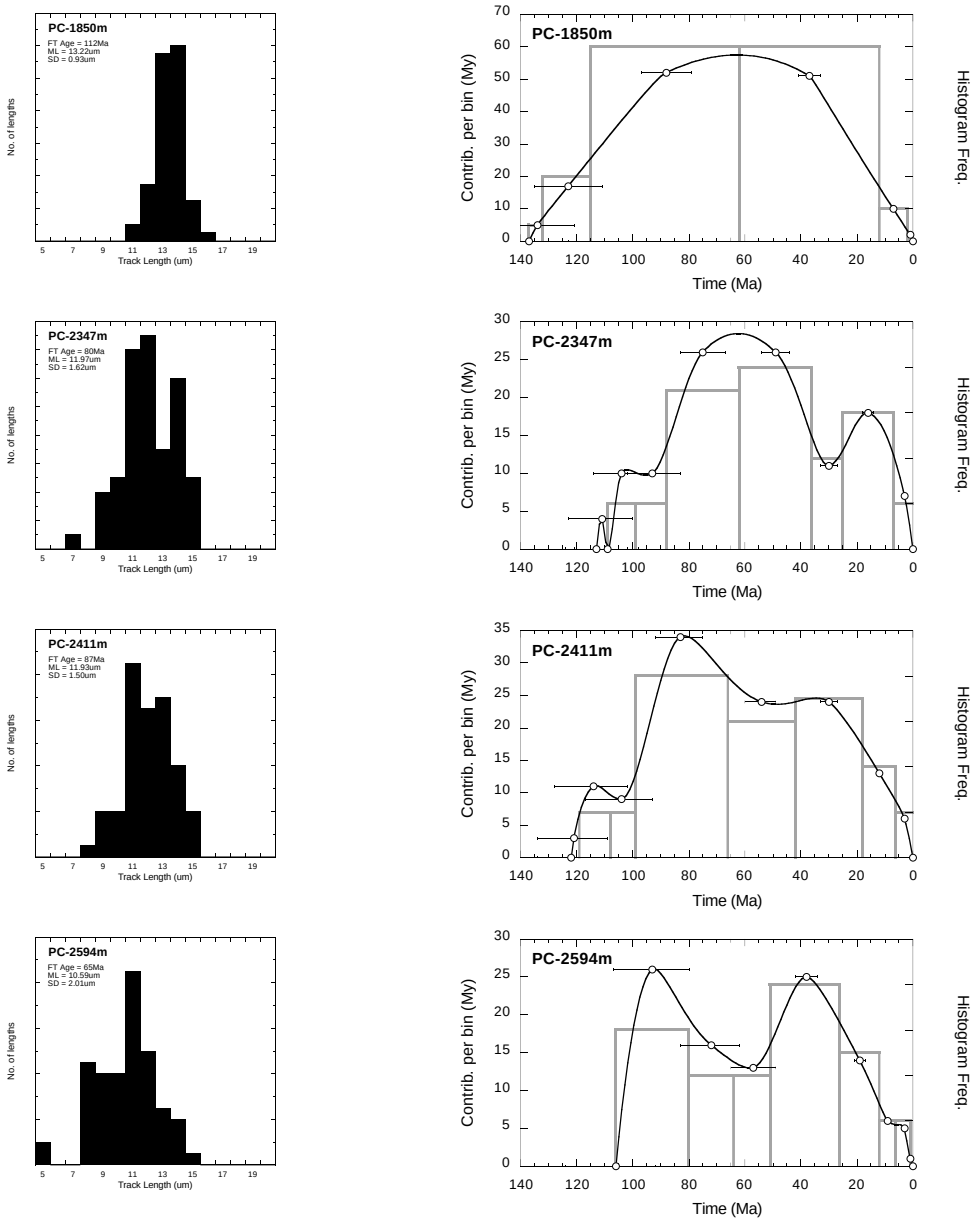

Figure 16 Port Campbell-4 well, Otway Basin, Australia. Track age spectra for four samples recovered from depths between between 1800m and 2600m outlined in Table 3 (Original data from Gleadow et al. 1986b).

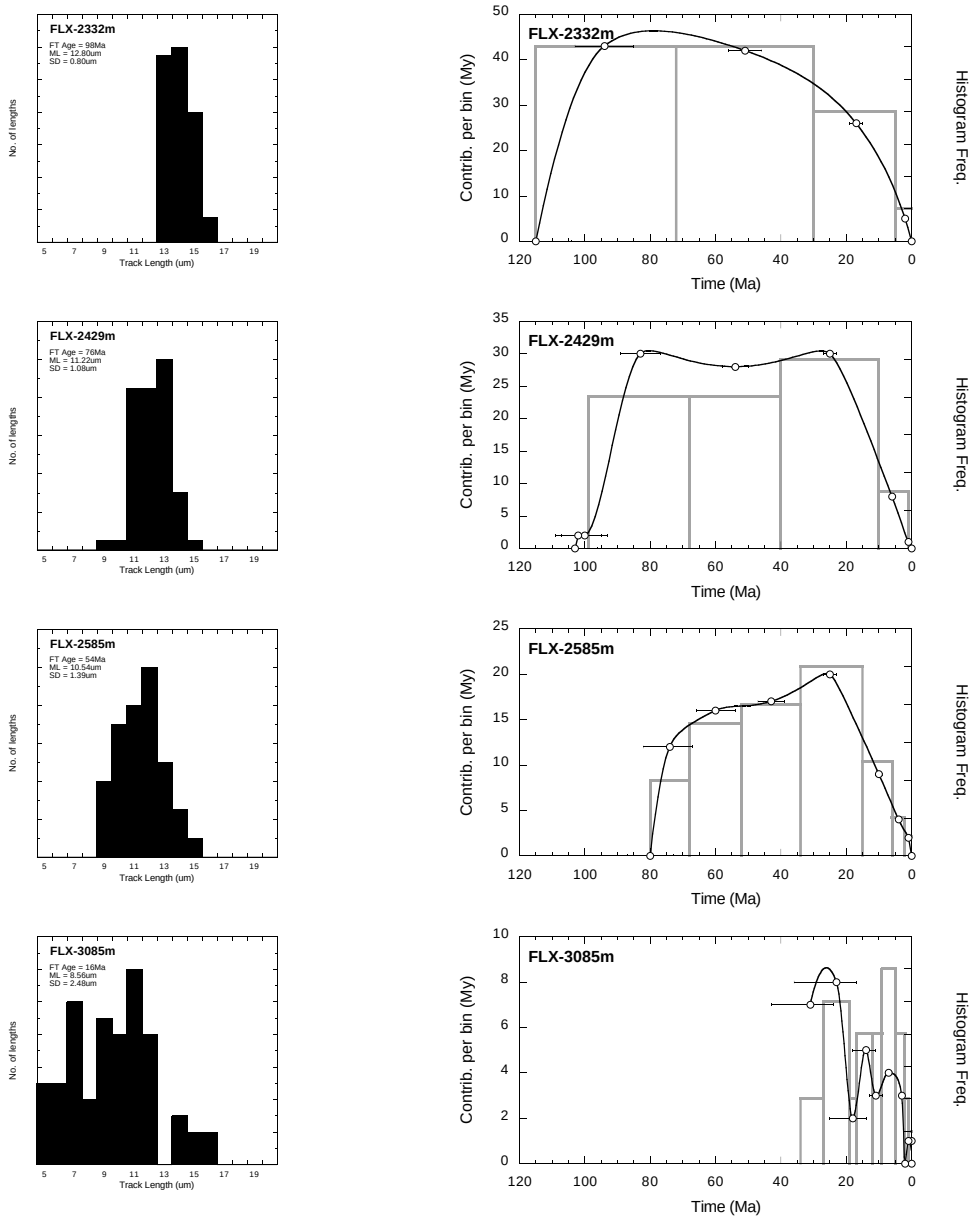

Figure 17 Flaxmans-1 well, Otway Basin, Australia. Track age spectra for four samples recovered from depths between between 2300m and 3100m outlined in Table 3 (Original data from Gleadow et al. 1986b).

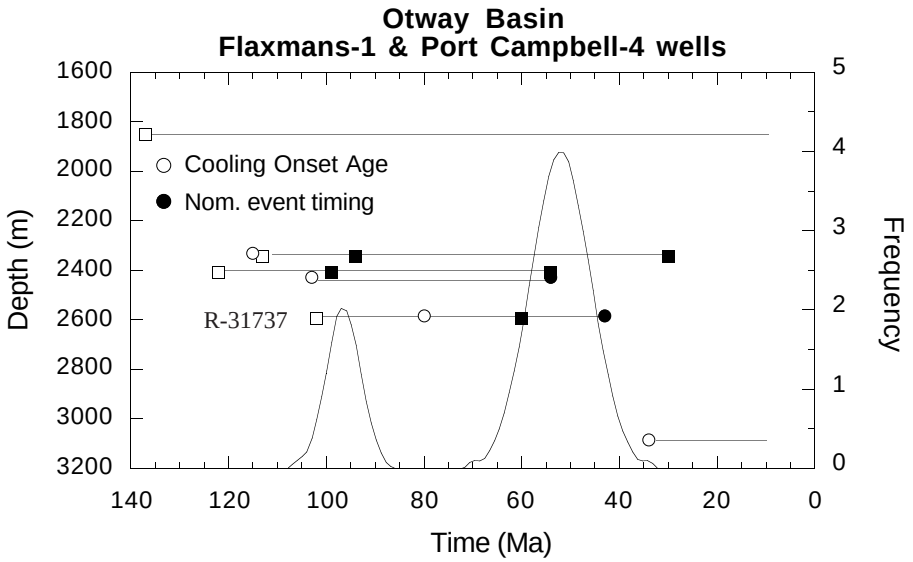

Figure 18 Composite event spectrum for Otway Basin wells showing events at ~95Ma and ~50Ma in the Port Campbell-4 well (circles), whereas only the later event is recorded in the Flaxmans-1 samples (squares). Overlain on this is an age-elevation plot based on "cooling onset" ages, and nominal event timing.

>90ºC), the samples show cooling onset ages significantly reduced from the stratigraphic age, indicating the loss of early tracks and resetting of the ages. Since both samples have "cooling onset" ages less than 90Ma, neither records the Cenomanian event, and only FLX-2585m records the Eocene event. In contrast, the deeper sample (FLX-3085m) did not cool sufficiently to start retaining tracks again until the early Oligocene.

The composite event spectrum for these two Otway Basin wells (Fig. 18) summarises the interpretations above, and it can be seen that neither the uppermost (stratigraphic age) sample nor the lowest (fully reset) sample record indications of tectonic events since the Early Cretaceous. The partially reset samples in between clearly retain the bulk of the information.

1.7.3 Zircon FT in thermobarometry and metamorphism (Brix et al. 2002)

As a final example of the broad utility of the TASC approach, an analysis was carried out on one of the few fission track studies for which confined track lengths in zircons have been published. Brix et al. (2002) applied a variety of thermobarometric techniques as well as zircon fission track anlaysis in order to establish the metamorphic conditions in a series of exhumed subduction fragments on the Mediterranean island of Crete. This island lies in an extraordinary tectonic setting and is a region of the Hellenic subduction zone that marks the boundary between the African and Eurasian plates. Rocks of the Phyllite-Quartzite Unit are characterised by high pressure-low temperature metamorphism, that reached temperatures of ~400ºC at about 24Ma.

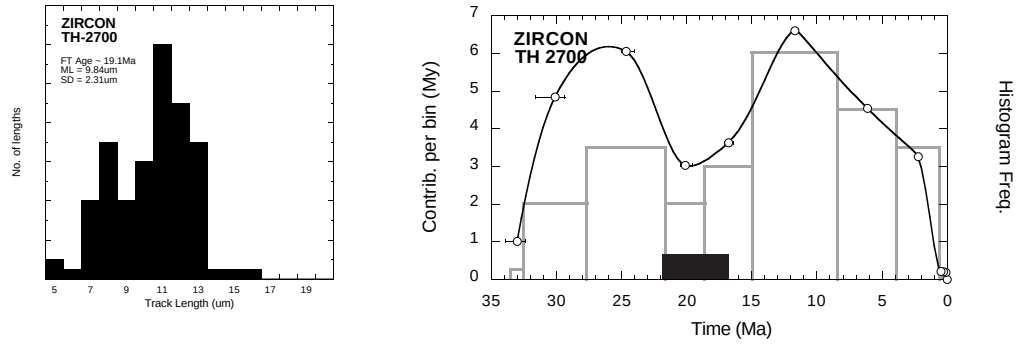

Figure 19 Length histogram and track age spectrum for Zircon FT sample TH-2700 (Brix et al. 200X). This sample has a cooling onset age of 34Ma and the spectrum suggests it reached maximum temperature during reheat at between 22-18Ma followed by rapid cooling at ~15Ma.

The spectrum shown in Fig. 19 was calculated using an inital track length (l_o) of 15µm, and is based on an original histogram comprising only those lengths with an angle to the c-axis of >60ºC (Brix et al. 2002). It should be noted here that the uncertainties attributed to the age contribution curve are those for apatite anisotropy and are probably far too optimistic for zircon. The initial length (l_o) chosen differs from the laboratory studies in zircon annealing by (Tagami et al., 1998), but was chosen on the basis of the typical maximum lengths measured by Brix and colleagues (2002). In practice, variation of this length (l_o) for these samples by 1-2µm makes only a small difference to the timing of length bins in the spectrum and no difference to the interpretation.

Within the limitations outlined, sample TH-2700 (Fig. 19) is interpreted as follows. The sample appears to have passed through the base of the zircon PAZ at around 34Ma, and cooled in a linear fashion until ~25Ma, at which time burial/reheating has significantly shortened the track population. Following the reheating event, the sample was subject to rapid cooling to upper levels of the ZPAZ before ~15Ma, at which time much more modest cooling rates were established.

This interpretation parallels the conclusions drawn by Brix et al (2002), who argued that the rocks of the Phylite-Quartzite Unit achieved peak thermal conditions at around 22Ma, and contrary to their expectations, had cooled through the ZPAZ at 15Ma.

1.8 Conclusions

Length-calibrated fission track ages, and their application in the track age spectra calculation (TASC) described here builds on the traditional age equation, long-applied in the fission track technique. By utilising all the available information in the track length histogram to calculate the nominal age of individual fission tracks, a robust estimate of the

age of the oldest track in a given sample can be extracted. A clear, visual indication of the age of "cooling onset" and timing of thermal perturbations can be plotted using the timeline against which the traditional length histogram has been constructed. Thus the thermal and temporal significance of each individual bin in the length histogram is clearly established. Although subject to the effects of annealing anisotropy, a conservative assessment of the uncertainties involved is given in the results. TASC does not require chemistry and mineralogical parameters and since the calculation is based on the raw data collected as part of fission track analysis, the results are completely independent of artifacts that may arise from assumptions in empirical annealing models.

When used in conjunction with the traditional length histograms (Fig. 20), the track age spectrum provides a powerful new tool for determining both the timing and style of a samples thermal history, and in some cases the plot gives an indication of the severity and rapidity of a thermal perturbation. The approach may also prove of significant value in the study of other minerals such as zircon, where annealing models are still evolving.

When applied to vertical profiles, TASC analysis enables rapid identification of events recorded both above and below a "break in slope". Estimates of exhumation rates (particularly above a "break in slope"), can be derived from "onset cooling ages and avoid the non-unique timing of traditional apparent fission track ages.

Semiquantitative timing information extracted from the track age spectra of grouped samples (eg. vertical profiles or localised tectonic blocks) can be effectively and concisely summarised on the event spectum in much the same way as detrital zircon age populations are illustrated in probability plots (Brandon, 1996). This enables the user to readily identify important thermal events at one site and is a powerful means of evaluating the regional thermal histories.

By itself, the "cooling onset" age can be used as the basis of extended regional contour maps giving a large-scale overview of regional cooling histories. In contrast to traditional maps relying on apparent fission track ages, the cooling onset age provides an unambiguous indicator of the time a sample entered the base of the PAZ. With some additional assumptions regarding composition and cooling rates, this information can be inverted to derive exhumation values for large areas.

The TASC approach should prove to be a powerful precursor to current well-established inverse modelling techniques. It cannot replace these methods but will complement them, so that in many cases the additional information garnered from TASC will enable robust model histories to be rapidly developed, particularly in areas where stratigraphic and structural control may be absent.

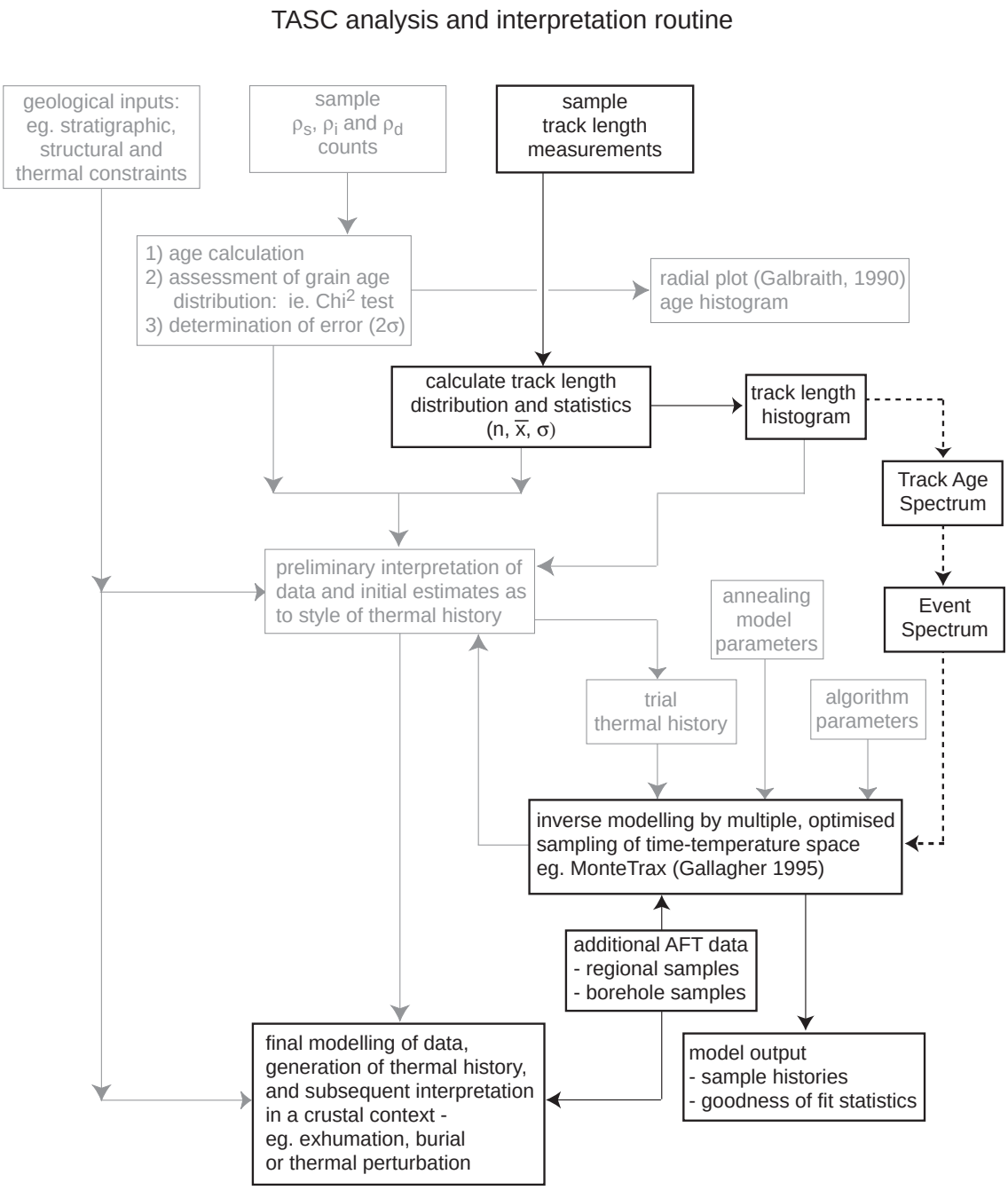

Figure 20. Modified version of the flow chart summarising conventional analysis and interpretation routine for apatite fission track thermochronology incorporating the TASC approach.

1.8 Acknowledgements

This work was made possible through the generous support of the Australian Research Council and the Australian Institute for Nuclear Science and Engineering.

1.9 References

Barbarand J, Carter, A, WoodI, Hurford AJ (2003). Compositional control of fission track annealing in apatite. Chem Geol 198:107-137.

Boellstroff J (1981). Are corrected fission -track ages correct? Nucl Tracks 5:230-232.

Brix MR, Stöckhert B, Seidel E, Theye T, Thomson SN, Küster M (2002). Thermobarometric data from a fossil zircon partial annealing zone in high pressure-low temperature rocks of eastern and central Crete, Greece. Tectonophys 349:309-326.

Burtner RL, Nigrini A, Donelick RA (1994). Thermochronology of Lower Cretaceous source rocks in th e Idaho-Wyoming thrust belt. AAPG Bull 78:1613-1636.

Carlson WD, Donelick RA, Ketcham, RA (1999) Variability of apatite fission-track annealing kinetics: I. Experimental results. Am Mineral 84:1213-1223.

Carpena J, Mailhe D, Poupeau G and Vincent D (1981) Model ages in fission track dating. Nucl Tracks 5:240-242.

Chaillou D, Chambaudet A (1981). Isothermal plateua method for apatite fission track dating. Nucl Tracks 5:181-186.

Corrigan J (1991) Inversion of apatite fission track data for thermal history information. J Geophys Res 96(B6):10374-10360.

Crowley KD (1985) Thermal significance of fission-track length distributions. Nucl Tracks 10(3):311-322.

Crowley KD (1993) Lenmodel – a forward model for calculating length distributions and fission-track ages in apatite. Comp Geosci 19(5):619-626.

Crowley KD, Cameron M, Schaffer LR (1991) Experimental studies of annealing of etched fission tracks in fluorapatite. Geochim Cosmochim Acta 55:1449-1465.

Dodson MH (1973) Closure temperature in cooling geochronological and petrological systems. Contr Mineral and Petrol 40:259-274.

Donelick RA (1991). Crystallographic orientation dependence of mean etchable fission track length in apatite: An empirical model and experimental observations. Am Min 76:1449-1456 .

Donelick RA, Ketcham AR, Carlson WD (1999). Variability of apaitite fission-track annealing kinetics: II. Crystallographic orientation effects. Am Min 84:1224-1234.

Donelick RA, Roden MK, Mooers JD, Carpenter BS, Miller DS (1990) Etchable length reduction of induced fission tracks in apatite at room temperature (~23°C): crystallographic oreintation effects and "initial" mean lengths. Nucl Tracks Radiat Meas 17(3):261-265.

Duddy IR (2000). The Otway Basin: geology, sedimentology, AFTA thermal history reconstruction and hydrocarbon prospectivity. Field trip guide for the 9th International Conference on Fission Track Dating and Thermochronology, Lorne Australia Feb 2000.

Fleischer RL, Price PB, Walker RM (1975) Nuclear Tracks in Solids: Principles and Applications. University of California, Berkeley. 605 pp.

Galbraith RF, Laslett GM, Green PF, Duddy IR (1990). Apatite fission track analysis: geological thermal history analysis based on a three-dimensional random process of linear radiation damage. Phil. Trans. Soc. Lond. 332:419-438.

Gallagher K (1995) Evolving temperature histories from apatite fission-track data. Earth Planet Sci Lett 136:421-435.

Gleadow AJW, Duddy IR (1981) A natural long-term annealing experiment for apatite. Nucl Tracks 5(1-2): 169-174.

Gleadow AJW, Duddy IR, Green PF, Hegarty KA (1986a). Fission track lengths in the apatite annealing zoneanf the interpretation of mixed ages. Earth Planet Sci Lett 78:245-254.

Gleadow AJW, Duddy IR, Green PF, Lovering JF (1986b). Confined fission track lengths in apatite - a diagnostic tool for thermal history analysis. Contrib Min Pet 94:405-415.

Gleadow AJW, Fitzgerald PG (1987). Uplift history and structure of the Transantarctic Mountains: new evidence from fission track dating of the basement apatites in the Dry Valleys area, southern Victoria Land. Earth Planet Sci Lett. 82:1-14.

Green PF (1980). On the cause of shortening of spontaneous fission tracks in certian mineral Nucl Tracks 4:91-100.

Green PF (1988) The relationship between track shortening and fission track age reduction in apatite: combined influences of inherent instability, annealing anisotropy, length bias and systems calibration. Earth Planet Sci Lett 89:335-352.

Green PF, Duddy IR, Gleadow AJW, Tingate PR, Laslett GM (1986) Thermal annealing of fission tracks in apatite, 1. A qualitative description. Chem Geol Isot Geosci Sect 59:237-253.

Green PF, Duddy IR, Laslett GM, Hegarty KA, Gleadow AJW, Lovering JF (1989) Thermal annealing of fission tracks in apatite, 4. Quantitative modelling techniques and extension to geological timescales. Chem Geol Isot Geosci Sect 79:155-182.

Haack U (1972) Systematics in the fission track annealing of minerals. Contrib Mineral Petrol 35:303-312.

Hurford AJ (1990) Standardization of fission track dating calibration:Recommendation by the Fission Track Working Group of the I.U.G.S. Subcommission on Geochronology. Chem Geol Isot Geosci Sect 80:171-178.

Issler DR (1996) Optimizing time-step size for apatite fission-track annealing models. Comp Geosci 22:67-74.

James K, Durrani SA (1986). The effect of crystal composition on fission-track annealing and closure temperatures in geological minerals: implications for the cooling rates of terrestrial and extraterrestrial rocks. Nucl tracks 6:277-282.

Ketcham RA, Donelick RA, Donelick MB (2000) AFTSolve: A program for multi-kinetic modelling of apatite fission-track data. Geol Mater Res 2(1).

Lal D, Rajan RS, Tamhane A.S (1969) Chemical composition of nuclei of Z > 22 in cosmic rays using meteoric minerals as detectors. Nature 221:33-37.

Laslett GM, Gleadow AJW, Duddy IR (1984). The relationship between fission track length and track density in apatite. Nucl Tracks 9:29-38.

Laslett GM, Kendall WS, Gleadow AJW, Duddy IR (1982). Bias in measurement of fission-track length measurements. Nucl Tracks 6:79-85.

Lutz TM, Omar G (1991) An inverse method of modeling thermal histories from apatite fission-track data. Earth Planet Sci Lett 104:181-195.

Naeser CW, Faul H (1969) Fission track annealing in apatite and sphene. J Geophys Res 74:705-710.

Nagpaul KK, Mehta PP, Gupta ML (1974). Annealing studies on radiation damage in biotite, apatite and sphene and corrections to fission track ages. Pageoph. 12:131-139.

Storzer D, Wagner GA (1969). Correction for thermally lowered fission track ages in tektites. Earth Planet Sci Lett. 5: 463-468.

Wagner GA, Storzer D (1970) Die interpretation von spaltspurenalter (fission track ages) am beispiel von naturlichen glasern, apatite und zirkonen. Eclogae Geol Helv 63(1):335-344.

Wagner GA, Storzer D (1972). Fission track length reductions in minerals and the thermal history of rocks. Trans Amer Nucl Soc 15:127-127.